A globally sampled high-resolution hand-labeled validation dataset for evaluating surface water extent maps

Rohit Mukherjee[1,2,★]**, Frederick Policelli**[3,★]**, Ruixue Wang**[2]**, Elise Arellano-Thompson**[2]**, Beth Tellman**[2]**,
Prashanti Sharma**[2]**, Zhijie Zhang**[2]**, and Jonathan Giezendanner**[1,4]

[1]Pacific Northwest National Laboratory, Richland, WA, United States of America
[2]University of Arizona, Tucson, Arizona, United States of America
[3]NASA Goddard Space Flight Center, Greenbelt, Maryland, United States of America
[4]Massachusetts Institute of Technology, Cambridge, Massachusetts, United States of America
★These authors contributed equally to this work.

Correspondence: Rohit Mukherjee (rohitmukherjee@live.com)

Abstract. Effective monitoring of global water resources is increasingly critical due to climate change and population growth. Advancements in remote sensing technology, specifically in spatial, spectral, and temporal resolutions, are revolutionizing water resource monitoring, leading to more frequent and high-quality surface water extent maps using various techniques such as traditional image processing and machine learning algorithms. However, satellite imagery datasets contain trade-offs that result in inconsistencies in performance, such as disparities in measurement principles between optical (e.g., Sentinel-2) and radar (e.g., Sentinel-1) sensors and differences in spatial and spectral resolutions among optical sensors. Therefore, developing accurate and robust surface water mapping solutions requires independent validations from multiple datasets to identify potential biases within the imagery and algorithms. However, high-quality validation datasets are expensive to build, and few contain information on water resources. For this purpose, we introduce a globally sampled, high-spatial-resolution dataset labeled using 3 m PlanetScope imagery (Planet Team, 2017). Our surface water extent dataset comprises 100 images, each with a size of 1024×1024 pixels, which were sampled using a stratified random sampling strategy covering all 14 biomes. We highlighted urban and rural regions, lakes, and rivers, including braided rivers and coastal regions. We evaluated two surface water extent mapping methods using our dataset – Dynamic World (Brown et al., 2022), based on Sentinel-2, and the NASA IMPACT model (Paul and Ganju, 2021), based on Sentinel-1. Dynamic World achieved a mean intersection over union (IoU) of 72.16 % and F1 score of 79.70 %, while the NASA IMPACT model had a mean IoU of 57.61 % and F1 score of 65.79 %. Performance varied substantially across biomes, highlighting the importance of evaluating models on diverse landscapes to assess their generalizability and robustness. Our dataset can be used to analyze satellite products and methods, providing insights into their advantages and drawbacks. Our dataset offers a unique tool for analyzing satellite products, aiding the development of more accurate and robust surface water monitoring solutions. The dataset can be accessed via https://doi.org/10.25739/03nt-4f29 (Mukherjee et al., 2024).

1   Introduction

Mapping surface water is becoming increasingly important due to the impacts of climate change, as many regions face the prospect of droughts (Dai, 2013) and floods (Tellman et al., 2021). Timely, accurate, and reliable monitoring of surface water extent is critical for better management, conservation, and risk-reduction practices, but this remains a growing challenge for researchers. Remotely sensed satellite data have provided a unique vantage point for measuring surface water extent (Bijeesh and Narasimhamurthy, 2020; Mueller et al., 2016) using different measurement principles such as optical and radar sensors (Markert et al., 2018). Recent advances in satellite sensors have increased spatial, spectral, and temporal resolutions, leading to significant growth in methods for monitoring surface water using multiple satellite products (Pekel et al., 2016; Martinis et al., 2022; Giezendanner et al., 2023). Among these methods, machine learning and deep learning algorithms gained popularity due to their ability to leverage large volumes of satellite data (both public and commercial) to accurately map the Earth's surface (Isik-dogan et al., 2017; Wieland et al., 2023).

However, the effectiveness of satellite water products based on different sensors is not consistent across all conditions, as each product involves trade-offs between spatial, spectral, and temporal resolutions (Wulder et al., 2015). Higher-spatial-resolution products like PlanetScope (PS) often produce more accurate maps than lower-resolution Sentinel-2 (10 m) or Landsat 8 (30 m) data (Acharki, 2022). Moreover, radar and optical sensors measure surface water properties differently, leading to variations in accuracy and suitability (Martinis et al., 2022), even at similar spatial resolutions. The study by Ghayour et al. (2021) compared Landsat 8 and Sentinel-2 and found performance varied across methods. As Wolpert (2002) asserted, no single algorithm is expected to perform optimally in every situation. The study by Li et al. (2022) summarizes the current common methods of water extraction based on optical and radar images.

Independently evaluating satellite products and methods using independent validation datasets is crucial for increasing trust in the results (Bamber and Bindschadler, 1997). However, such datasets are resource-intensive to create, and existing ones may not be suitable for all needs. For example, BigEarthNet (Sumbul et al., 2019) contains around 600 000 multi-labeled Sentinel-2 image patches, of which 83 000 contain water bodies. This dataset confirms the presence of water within a patch but does not delineate it at the pixel level. The Chesapeake Conservancy land cover dataset (Chesapeake Bay Program, 2023) provides high-resolution (1 m) per-pixel water labels for the Chesapeake Bay watershed regional area. LandCoverNet (Alemohammad and Booth, 2020) contains global 10 m resolution data from Sentinel-2 with a water class. Flood mapping has also been a strong research focus, with datasets like the Sentinel-1-based NASA flood detection (Gahlot et al., 2021), Sen1Floods11

(Bonafilia et al., 2020), Sen12-Flood (Rambour et al., 2020), and C2S-MS Floods (Cloud to Street et al., 2022) that use both optical (Sentinel-2) and radar (Sentinel-1) imagery. While suitable for validating surface water maps, some of these datasets rely on 10 m resolution public satellite imagery or lack global coverage at high resolution. The ephemeral nature of floods also requires specialized detection models even though floodwater is technically surface water (Bonafilia et al., 2020). Wieland et al. (2023) developed a semiautomated global binary surface water reference dataset with 15 000 tiles (256×256 pixels) sampled from high-resolution (≤ 1 m) imagery. However, this dataset uses weak labels generated by a model rather than manual labeling, making it less suitable for validation.

To thoroughly evaluate a product's effectiveness and robustness, multiple independent assessments are needed since high accuracy on one dataset does not guarantee similar performance on others. No single dataset can fully represent the real world (Paullada et al., 2021), and manual labels inevitably contain some subjectivity (Misra et al., 2016). Independent evaluations also help mitigate the issue of data leakage, where the validation set is improperly used during model training, leading to overfitting (Vandewiele et al., 2021). Multiple independent validation datasets are therefore essential for comprehensively evaluating and building trust in remote sensing-based surface water products and methods.

In this study, we present a high-quality, globally sampled, high-resolution surface water dataset consisting of 100 hand-labeled 1024×1024 pixel PlanetScope images at 3 m resolution. Our work builds upon existing satellite-based datasets for validating surface water extent. The motivation is to provide a higher-resolution hand-labeled dataset for evaluating surface water products derived from medium-resolution public satellites like Landsat and Sentinel and commercial higher-resolution PlanetScope imagery. Our dataset addresses some of the limitations of existing datasets by providing pixel-level water labels at a higher resolution (3 m) compared to some other datasets and encompassing diverse biomes and contexts (urban/rural, mountains/plains, rivers/lakes) for comprehensive evaluations. We evaluate two state-of-the-art surface water extent mapping methods using our dataset: the Dynamic World land use and land cover product based on optical Sentinel-2 imagery and the NASA IMPACT inundation mapping model based on radar Sentinel-1 data, which was the winning solution in a recent flood detection challenge. By applying our validation dataset to these products and methods, we aim to better understand their advantages and limitations. We anticipate our dataset will contribute to improved accuracy assessment, spatial generalizability analysis, and robustness evaluation of existing surface water products and methods. These advancements can ultimately benefit societies by promoting more effective monitoring and management of water resources, especially in the face of climate change and population growth.

2 Data preparation

2.1 Sampling

Our objective was to build a dataset that closely represents the true distribution of surface water features using only 100 samples. A representative dataset enables testing the spatial generalizability and accuracy of surface water extent products. However, achieving a true representation is nearly impossible (Paullada et al., 2021). We approached this challenge by sampling from different biomes, as defined by Olson et al. (2001), which encompass various climates and land conditions, giving a better chance of providing high variance within samples.

We employed a stratified random sampling strategy to ensure the representativeness of our dataset. First, we created a 2 km buffer around global river and lake shapefiles provided by the World Wildlife Fund (2005) using QGIS (Quantum GIS). We then clipped these buffers with the shapefiles of each of the 14 biomes. Within each biome, we randomly placed 50 points using QGIS's random point generator and selected at least 5 of them as samples.

To address the various contexts in which surface water exists, we randomly selected additional samples from urbanized regions (Patterson and Kelso, 2012), braided rivers, and coastal regions. Urban areas are spatially heterogeneous, often resulting in increased complexity for water detection. We also separately sampled from lakes and rivers to ensure a balanced representation of both water body types. Braided rivers and coastal areas were included.

Figure 1 shows the number of samples for each biome, while Fig. 2 illustrates the global spatial distribution of the samples. The numbers of samples from "Tropical and Subtropical Dry Broadleaf Forests" and "Tropical and Subtropical Coniferous Forests" were limited due to their smaller areal coverage. Approximately two-thirds of our labels are from rivers and the remaining one-third are from lakes. We sampled a larger portion from "Deserts and Xeric Shrublands" (16 samples) because water extraction methods generally perform worse in these regions, especially when using radar imagery (Martinis, 2017).

The temporal distribution of our samples spans from 2021 to 2023, covering different seasons to capture seasonal variations in surface water extent. While our sampling strategy aimed to maximize representativeness within the constraints of labeling resources, we acknowledge that the limited number of samples (100) may not fully capture all global surface water variations.

During the sampling process, we implemented quality control measures to ensure that the selected locations were suitable for labeling and analysis. We downloaded the PlanetScope scene for each location, divided the scene into 1024 × 1024 sized images, and then selected the image that contained sufficient water and no cloud cover.

2.2 Data processing

After selecting 100 locations based on our sampling strategy, we downloaded 8-band, 3 m resolution SuperDove PlanetScope (PS) imagery from 2021 to 2023 using our access to the NASA Commercial SmallSat Data Acquisition (CSDA) program. As our objective was to evaluate most medium-resolution satellite sensors, including Sentinel-1 (S1), we ensured that the failure of the Sentinel-1B satellite, on 23 December 2021, did not create a large temporal gap between the label and the last available scene from the satellite. For locations only covered by Sentinel-1B and not Sentinel-1A, we acquired PS scenes before the Sentinel-1B failure date.

During the scene selection process, we excluded areas with perennially frozen water. If a location contained seasonal ice, we replaced that PS image with a summer image when the water was not frozen. This approach ensured that our dataset focused on liquid water surfaces, which are more relevant for surface water extent mapping.

From each larger PS scene, we extracted a 1024 × 1024 pixel image, covering an area of approximately 9.4 km^2. We chose 1024 × 1024 pixel images to ensure sufficient pixels and spatial context for comparison with medium-resolution imagery (e.g., Landsat, Sentinel). For instance, a 30 m Landsat image corresponding to our labels would have around 100 × 100 pixels, while a 10 m Sentinel image would have approximately 376 × 376 pixels. Figure 3 showcases two examples of the PS images selected for labeling, displayed in false-color composite (near-infrared, red, and green bands).

2.3 Data labeling

We used high-resolution 3 m PlanetScope (PS) data for labeling, ideal for the evaluation of lower-resolution satellite products such as Sentinel-1 (S1), Sentinel-2 (S2) at 10 m, or Landsat sensors at 30 m.

The labeling was performed by experienced analysts to distinguish between three classes: water, low-confidence water, and non-water. The water class represents areas with a clear presence of water, while the low-confidence water class marks pixels where the presence of water is uncertain but probable. The non-water class encompasses all other land cover types. To assist the labelers, we provided true-color composite (TCC) and false-color composite (FCC) images using the near-infrared, red, and green bands for each sample.

In cases where the presence of water was unclear in the PS imagery, we cross-referenced them with higher-resolution basemaps from Bing and Google. Unresolved features were assigned to the low-confidence water category, ensuring that the water class only includes pixels with a high degree of certainty. During the evaluation process, the low-confidence water class can be excluded or added to the water category as necessary.
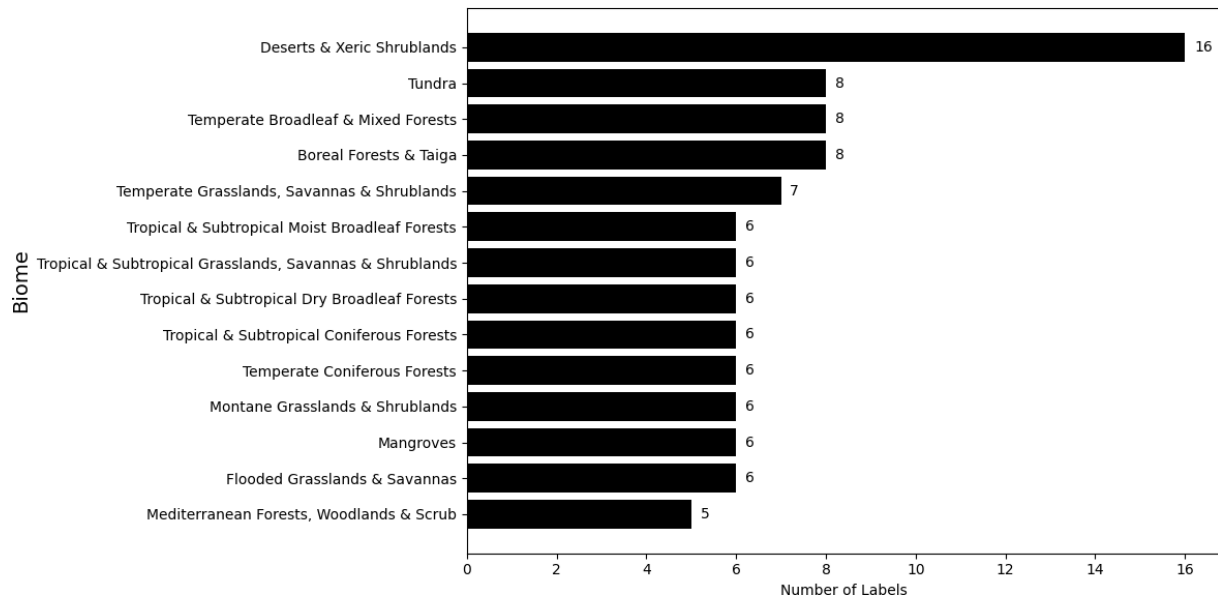
Figure 1. Distribution of sampled labels across different biomes. The bar chart illustrates the number of surface water labels collected from each of the 14 biomes defined by Olson et al. (2001). The sampling strategy aimed to ensure a balanced representation of surface water features across diverse ecological regions while accounting for the areal coverage of each biome.
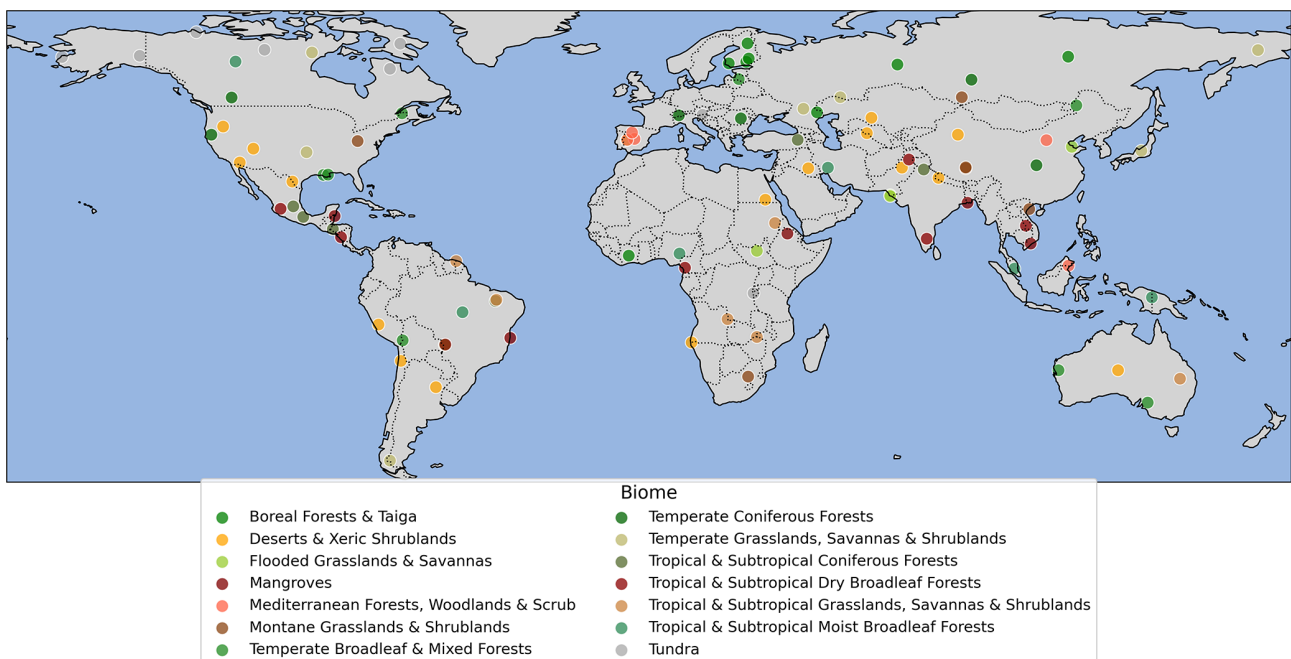

Figure 2. Global distribution of the 100 surface water labels sampled for the dataset. The map depicts the geographical locations of the sampled labels, which were sampled to represent diverse global biomes (refer to Table 1 for the number of labels per biome) and ensure a representative dataset of water features. The sampling approach also aimed to capture the variability of surface water features across urban areas, braided rivers, and coastal regions.

To streamline the labeling process and ensure the creation of high-quality labels, we utilized the Labelbox platform (Labelbox, 2024), which provides efficient tools for data annotation. After the initial labeling, we performed several rounds of quality checks on each label to maintain accuracy and consistency across the dataset.

In total, we labeled 100 images, each with a size of 1024×1024 pixels, covering a total surface area of $940\,\mathrm{km}^2$.
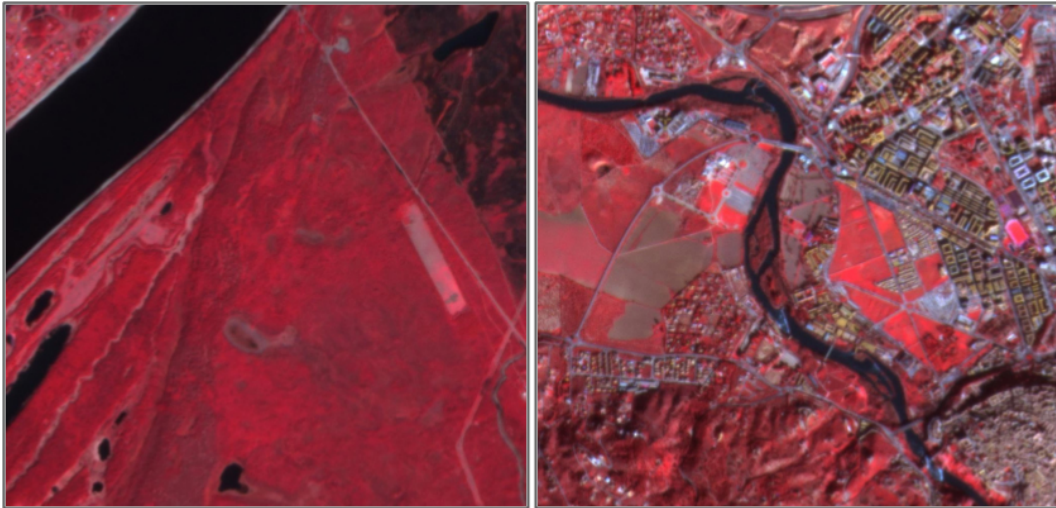
Figure 3. PlanetScope images selected for labeling are shown in false-color composite (near infrared, red, and green). Left: Vilyuy river, Republic of Sakha, Russia, SID09 (Image © Planet Labs PBC 2021); right: Tagus river, Toledo, Spain, SID17 (Image © Planet Labs PBC 2022).

The labeling process, including quality control, took approximately 2 h per image, resulting in a total of 200 h of work. The labeled surface water accounts for nearly 250 km^2 of the total area. Each label is assigned a unique sample ID (SID) ranging from 1 to 100 and includes the date (YYYYMMDD) of the PS image used for labeling.

2.4 Dataset analysis

We labeled a total of one-hundred 1024×1024 PS images at 3 m, with the overall class distribution covering 24.9 % of the total surface area, low-confidence water covering 1.2 %, and the rest (73.9 %) being non-water (Fig. 5). The distribution of water pixel percentages for each individual label, as displayed in Fig. 6, demonstrates that most labels contain less than 50 % water pixels by design, with the mean water surface area per label being 26.10 km^2. This focus on having more non-water area enables better delineation of water boundaries, as the water class itself tends to be more homogeneous and therefore less complex from both labeling and mapping perspectives.

As mentioned previously, our labeled dataset covers water surface areas across different biomes (Table 1). The mean percentage of water content per label varies substantially between biomes, from a low of 5.29 % for "Mediterranean Forests, Woodlands and Scrub" to a high of 42.95 % for "Temperate Grasslands, Savannas and Shrublands". This demonstrates the diversity of landscapes and water coverage captured in our dataset. In total, our dataset provides 2609.78 km^2 of labeled water surface area, covering a variety of landscapes such as rivers passing through urban regions, braided rivers in deltas, rivers passing through forests and agricultural fields, and waterbodies in plain and moun-

tainous regions. The diversity and representativeness of our dataset make it a valuable resource for testing the limits and robustness of satellite data products and mapping methods.

2.5 Dataset structure

All 100 labels are in the GeoTIFF format with the UInt8 data type and a single band. Each pixel can contain four possible values: 0 (no data), 1 (non-water), 2 (low-confidence water), and 3 (water). The labels are in the WGS84 (EPSG:4326) coordinate reference system. Each label has a corresponding PlanetScope image used for labeling in Labelbox. The PlanetScope images are also in the WGS84 (EPSG:4326) coordinate reference system and contain three spectral bands (red, green, and blue) in true-color composite. Based on our PS image release agreement with Planet, we converted the original surface reflectance values to byte format with possible pixel values between 0 and 255, instead of UInt16.

The label files are named using the following convention: SIDX_YYYYMMDD.tif, where "SIDX" is the unique sample ID (with X ranging from 1 to 100) and "YYYYMMDD" represents the date of the PlanetScope image used for labeling. The corresponding PlanetScope images follow the naming convention: SIDX_PSID.tif, where SIDX is the same as the label, but PSID is the original SuperDove PlanetScope image ID, allowing for the retrieval of the original surface reflectance values, provided there is access.

Our dataset is organized using the SpatioTemporal Asset Catalog (STAC) format, which is a standardized way to describe and catalog geospatial data. The STAC format provides a clear and consistent structure for storing and accessing the labels and their corresponding PlanetScope images, along with relevant metadata.
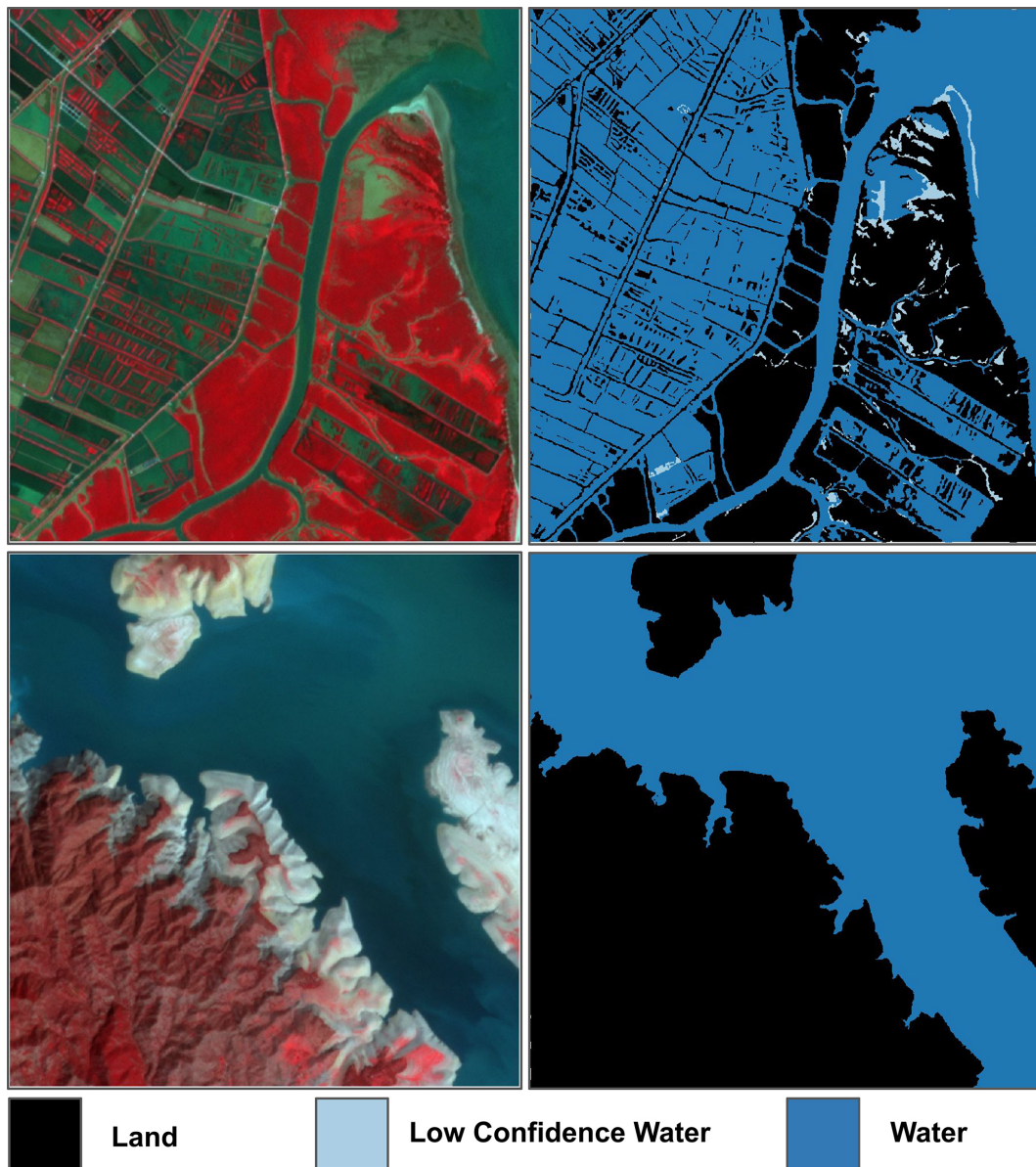
Figure 4. Examples of PlanetScope imagery and corresponding labels (top row: Dong Tranh River, Ho Chi Minh City, Vietnam (SID46); bottom row: Siran River, Pakistan (SID28)). The images are labeled with three categories: (1) non-water, (2) low-confidence water, and (3) water. The low-confidence water category marks pixels where delineating between water and non-water is not apparent, but the probability of water being present is moderately high. Image © Planet Labs PBC 2022.

3 Evaluating surface water mapping methods using our hand-labeled dataset

We evaluated two surface water mapping methods based on an optical and a radar satellite imagery product to demonstrate the use of our validation dataset. We used standard metrics for classification – precision, sensitivity, specificity, F1 score, intersection over union (IoU), and accuracy for evaluating the two surface water maps. We measured their performance across each biome and their overall performance.

3.1 Performance of Sentinel-2-based Dynamic World on detecting surface water

Dynamic World (DW) is a land use land cover product from Google that utilizes a deep learning model trained on their own labeled dataset. The product includes nine classes, including water, and produces a map for every Sentinel-2 image. Each Sentinel-2 image is post-processed and with clouds removed. We downloaded Sentinel-2 images within 3 d of each of the 100 labeled PlanetScope images. We also applied a not-a-number (NaN) filter, ensuring that images with
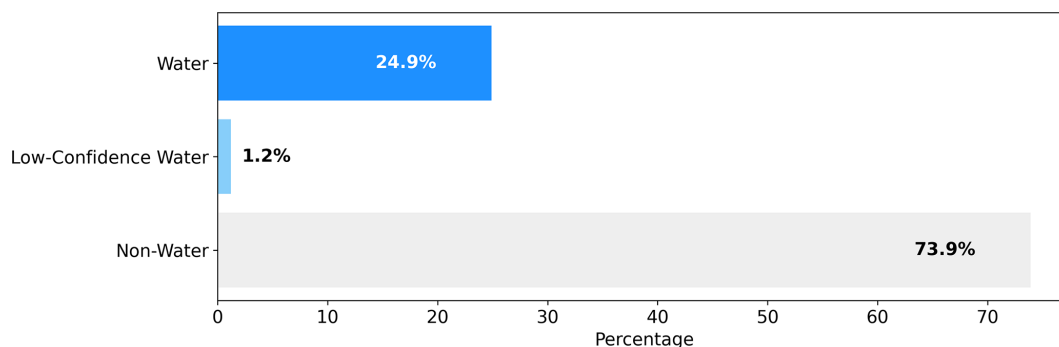
Figure 5. Class distribution across labels (non-water, low-confidence water, and water). The non-water class shares the largest percentage as it encompasses the water class. Low-confidence water pixels are only a minor percentage.
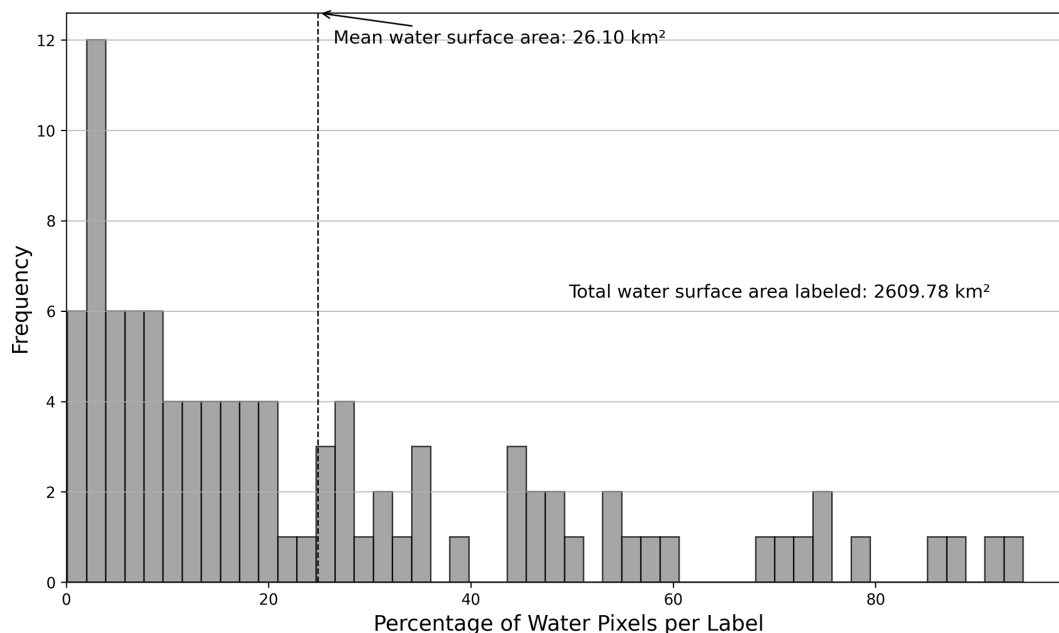

Figure 6. Distribution of water pixels per sample. The figure shows the percentage of water pixels within one sample. Most samples contain less than 50 % of water by design, as the focus is to delineate the boundaries since the water class is more homogeneous and, therefore, less complex.

at least 90 % valid pixels are considered. After applying the temporal and NaN filters, there were 53 corresponding Sentinel-2-based DW maps out of our 100 labels. From each DW map, we extracted the first band, which contains the water class. Each DW class contains continuous values between 0 and 1, where 1 denotes the highest confidence in the model prediction. We converted the continuous values to binary, thresholding at 0.3. The water class is one of the least confused classes in the DW product, so mixed pixels are less likely. Finally, we evaluated DW on our labels. Note that for evaluation we converted the low-confidence water class to water. We finally resampled the DW water class to match the resolution of the labels at 3 m using nearest-neighbor interpolation before evaluating. Note that for evaluation we merged

the low-confidence water class with water. Therefore, labels were either 0 (non-water) or 1 (water).

Figure 7 illustrates the performance of the water class in the Dynamic World product across different biomes using IoU. IoU provides an assessment of the overlap between the predicted and ground truth water pixels, with higher values indicating better performance. The number of samples per biome varies, with some biomes having more representative data than others. For biomes with a larger number of samples, such as "Deserts and Xeric Shrublands" and "Boreal Forests and Taiga", the IoU scores provide a more robust evaluation of the DW water class performance. Despite the variations in sample size, notable differences in performance can be observed among the biomes. It is important to note that the IoU metric is influenced by the amount of water present in each

Table 1. Mean percentage of water content per label across different biomes. The table shows the average proportion of water pixels within the labeled samples for each biome, highlighting the variability in water coverage across diverse ecological regions.

| Biome	Mean water content per label, %
Boreal Forests and Taiga	22.48
Deserts and Xeric Shrublands	18.96
Flooded Grasslands and Savannas	27.45
Mangroves	40.75
Mediterranean Forests, Woodlands and Scrub	5.29
Montane Grasslands and Shrublands	23.71
Temperate Broadleaf and Mixed Forests	19.48
Temperate Coniferous Forests	6.55
Temperate Grasslands, Savannas and Shrublands	42.95
Tropical and Subtropical Coniferous Forests	16.80
Tropical and Subtropical Dry Broadleaf Forests	20.71
Tropical and Subtropical Grasslands, Savannas and Shrublands	11.96
Tropical and Subtropical Moist Broadleaf Forests	27.39
Tundra	30.77
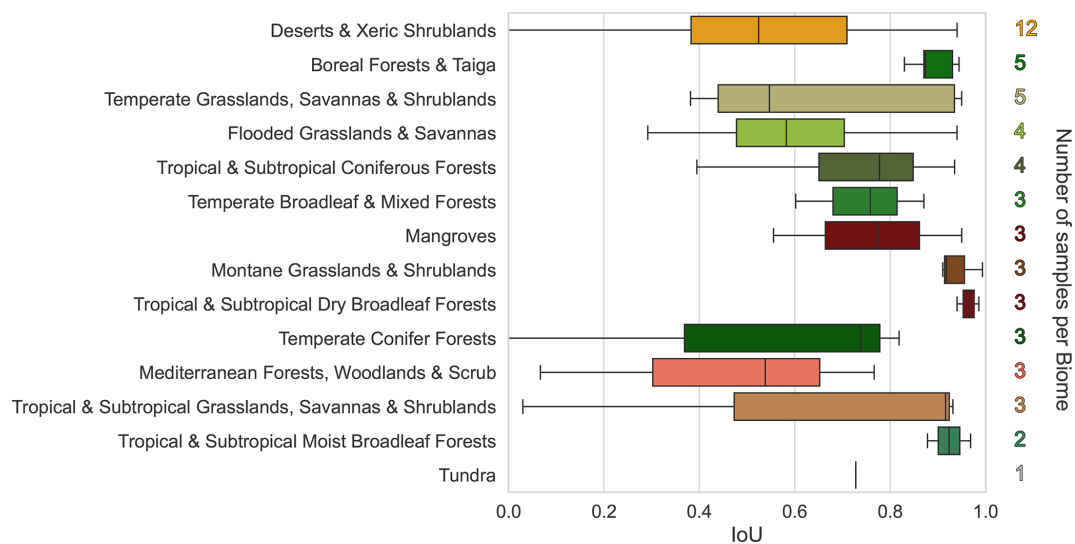
Figure 7. Intersection over union (IoU) performance of the Dynamic World (DW) water class across different biomes. The number of samples per biome is shown on the right of each bar. Higher IoU scores suggest better performance in detecting surface water. The error bars represent the standard deviation of IoU scores within each biome.

label. Higher water percentage often leads to higher IoU. However, our dataset has an average of 26.1 % surface water pixels, providing a balanced assessment of the DW water class performance.

Figure 8 provides a visual comparison of the Dynamic World water class predictions with the labels for two locations: Sundarban National Park, Bangladesh (SID01), and Shandong, China (SID13). The DW product appears to capture the majority of the water pixels accurately; however, it misses the narrow rivers (SID01) and it incorrectly ignores two bridges (SID13).

Table 2 summarizes the performance metrics for the Dynamic World water class evaluated on our hand-labeled

Table 2. Performance metrics for the Dynamic World (DW) water class evaluated on our hand-labeled dataset. The table presents the mean and standard deviation of various metrics. IoU denotes intersection over union. Higher values indicate better performance.

Metric	Mean	SD
Precision	0.8812	0.2301
Sensitivity	0.7745	0.2830
Specificity	0.9656	0.0888
F1 score	0.7970	0.2623
IoU	0.7216	0.2763
Accuracy	0.9529	0.0542

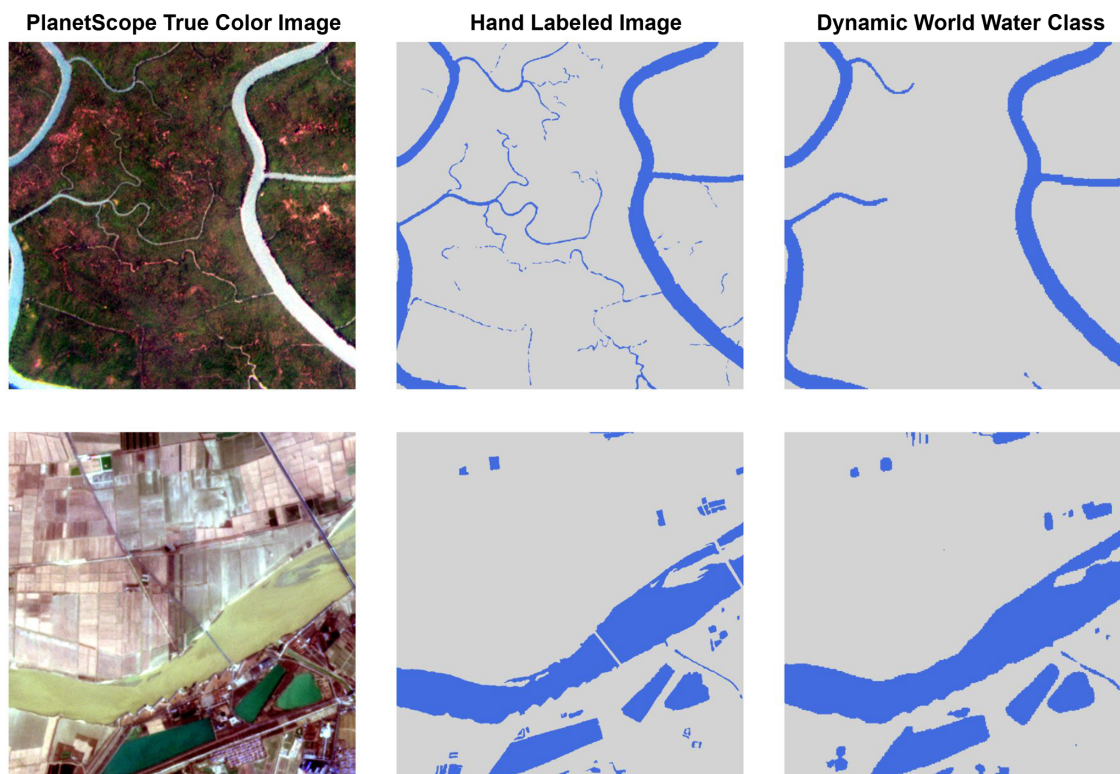| PlanetScope True Color Image	Hand Labeled Image	Dynamic World Water Class

Figure 8. Comparison of a PlanetScope true-color image (left), the corresponding hand-labeled image (middle), and the Dynamic World water class prediction (right). Top: Sundarban National Park, Bangladesh (SID01); bottom: Shandong, China (SID13). Image © Planet Labs PBC 2022.

dataset. The mean precision of 0.8812 indicates that, on average, 88.12 % of the pixels predicted as water by DW are actually water in our ground truth labels. The mean sensitivity (recall) of 0.7745 suggests that DW correctly identifies 77.45 % of the water pixels in our labels. The high mean specificity (0.9656) indicates that DW accurately classifies non-water pixels, with minimal misclassification as water. The F1 score, which is the harmonic mean of precision and recall, has a mean value of 0.7970, indicating a good balance between the two metrics. The mean IoU of 0.7216 signifies that, on average, there is a 72.16 % overlap between the predicted and ground truth water pixels. Lastly, the mean accuracy of 0.9529 shows that DW correctly classifies 95.29 % of the pixels overall, including non-water pixels. However, the high standard deviation indicates that there is a large variability in performance for almost all metrics except specificity and accuracy, since they take into account the non-water pixels.

3.2 Performance of the Sentinel-1-based deep learning model

We evaluated the performance of a deep learning model (Paul and Ganju, 2021) for inundation mapping that uses S1 radar imagery. This deep learning model was the competition win-

ner at the NASA IMPACT challenge for flood detection. Unlike Dynamic World, which contained a surface water class, this method focuses on flood or more specifically inundation class. Technically, our hand-labeled dataset also labels inundation, although our labels did not focus on capturing flooding. Therefore, we are not directly comparing the S1 IMPACT flood model against the Dynamic World water class.

We processed radiometrically corrected S1 imagery from Alaska Satellite Facility (ASF)'s data repository using the Hyp3 API (application programming interface). S1 imagery was searched for each label 3 d before and after the labeled date. We clipped the S1 scenes based on the labels, and then we applied the trained model to these clipped S1 scenes using the trained model. We then evaluated the predictions from the deep learning model on our labels after resampling the imagery to match the resolution of the higher-resolution labels using nearest-neighbor interpolation. Thus, 72 S1 images were selected for this evaluation. Note that for evaluation we converted the low-confidence water class to water. Therefore, labels were either 0 (non-water) or 1 (water).

Figure 9 illustrates the performance of the S1-based deep learning model across different biomes using the intersection over union (IoU) metric. Performance across biomes has a large variation, with some notable differences. For example, the IMPACT model performed robustly on "Tropi-
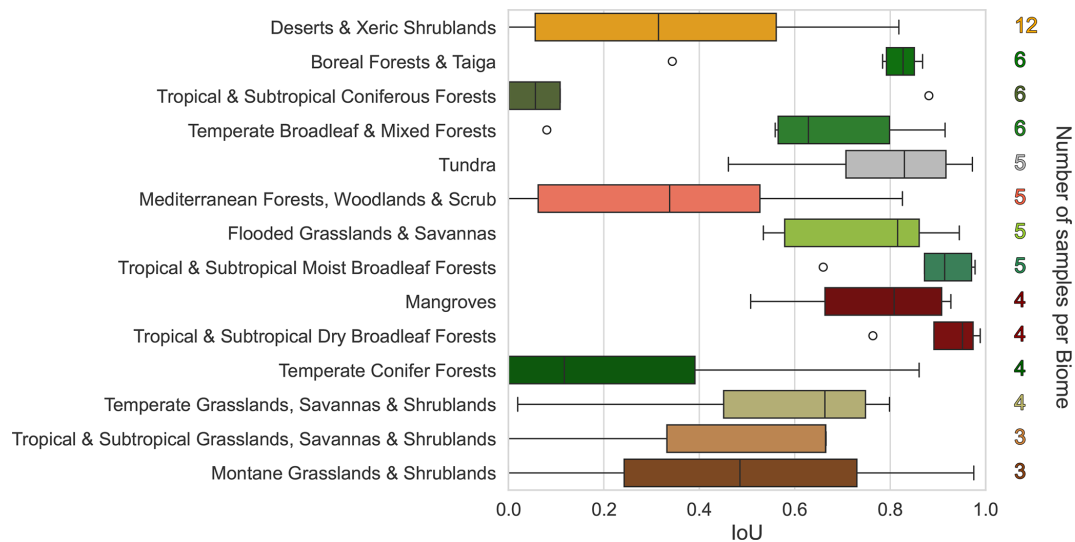
Figure 9. Intersection over union (IoU) performance of the Sentinel-1-based deep learning model across different biomes. The number of samples per biome is on the right of each bar. Higher IoU scores suggest better performance in detecting surface water. The error bars represent the standard deviation of IoU scores within each biome.

cal and Subtropical Dry Broadleaf Forests", "Tropical and Subtropical Moist Broadleaf Forests", "Tundra", and "Mangroves". Although for "Tropical and Subtropical Coniferous Forests", "Temperate Coniferous Forests", and "Deserts and Xeric Shrublands", the model performed less accurately and with large variations; this was especially true for "Mediterranean Forests, Woodlands and Scrub" where the model consistently performed poorly. The effectiveness is influenced by the fact that the training dataset of this model is focused on only five flood events globally. Therefore, performing accurately on the global surface water dataset is not the objective of this model. Nonetheless, the objective is still detection inundation, and the variation in performance provides clues to how such a model can be improved by sampling from biomes or other contexts (urban, river, lake, etc.).

Figure 10 provides a visual comparison of the Sentinel-1-based deep learning model's predictions with the ground truth labels for two locations: Nam Định, Vietnam (SID33), and Paymaster Landing, California, USA (SID59). The model appears to capture the majority of the water pixels accurately. However, the labels and the corresponding prediction by the S1-based model demonstrates the complexity of labeling and identifying water in a meandering braided river (SID33). In the case of SID59, the S1 model performs well, except for the coarser edges of a river in a more arid landscape.

Table 3 summarizes the performance metrics for the S1-based deep learning model evaluated on our hand-labeled dataset. The metrics exhibit significant variability across the evaluated labels. The S1 IMPACT model generally found it difficult to predict water pixels across several biomes. Apart from the differences in resolution, turbulent water and wa-

Table 3. Performance metrics for the Sentinel-1 (S1) IMPACT flood detection model evaluated on our hand-labeled dataset. The table presents the mean and standard deviation of various metrics. IoU denotes intersection over union. Higher values indicate better performance.

Metric	Mean	SD
Precision	0.6547	0.3488
Sensitivity	0.7485	0.3408
Specificity	0.8653	0.2309
F1 Score	0.6579	0.3435
IoU	0.5761	0.3406
Accuracy	0.8734	0.1922

ter located in spatially heterogeneous landscapes are more complicated to detect. Given the cloud-free observations, S1-based models can be of considerable benefit for regular monitoring and consistent observations.

4 Limitations

Although our hand-labeled dataset provides a valuable resource for evaluating surface water extent products, it has several limitations that must be considered. First, the spatial resolution of the dataset is limited to 3 m, making it more suitable for evaluating lower-spatial-resolution imagery (> 3 m). For higher resolutions (≤ 3 m), the influence of human labeling errors on the evaluation results is likely to increase. Despite our efforts to cross-reference multiple sources of higher resolution (< 1 m Bing and Google basemaps) during our labeling process and implement con-
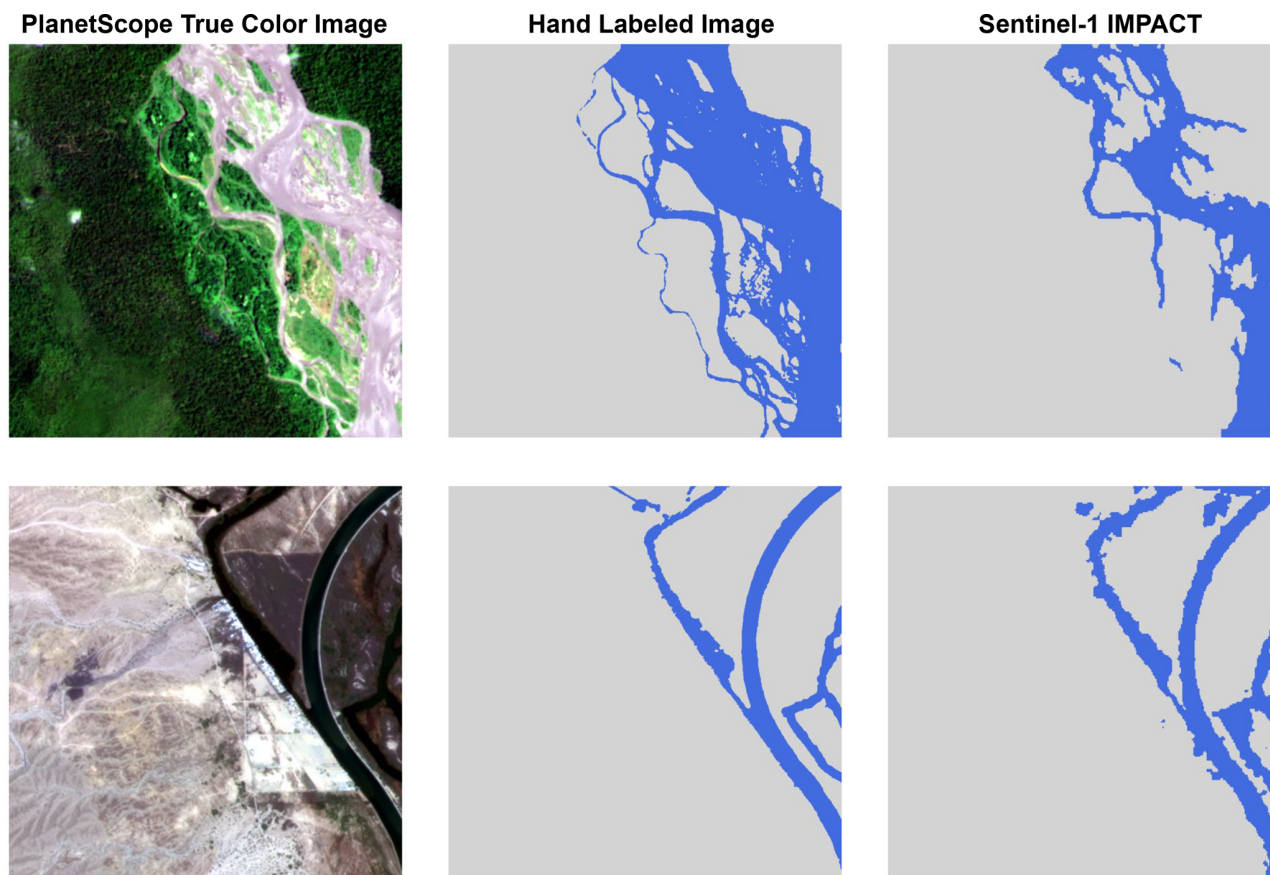
PlanetScope True Color Image	Hand Labeled Image	Sentinel-1 IMPACT

Figure 10. Comparison of a PlanetScope true-color image (left), the corresponding hand-labeled image (middle), and the surface water predictions of the Sentinel-1-based deep learning model (right). Top: Nam Định, Vietnam, SID33 (Image © Planet Labs PBC 2021); bottom: Paymaster Landing, California, USA, SID59 (Image © Planet Labs PBC 2022).

siderable quality control, the dataset unavoidably contains biases from our labelers, in addition to the biases in the optical PS imagery itself. A model using PS will likely perform the best since PS was the primary source for labeling. Moreover, some features remained unresolved, especially features finer than 3 m, leading to the addition of another class called "low-confidence water".

While we made an effort to include samples from diverse contexts in which water can be found (urban, lakes, braided rivers, mountainous regions) and multiple biomes covering different seasons, designing a truly representative dataset is not feasible. The stratified random sampling strategy used to create the dataset aims to cover diverse contexts and biomes but may not capture all the variability in surface water appearance across different regions and seasons. Additionally, the dataset only represents a snapshot in time and does not account for temporal changes in surface water extent, which can be significant in some regions due to seasonal variations, human interventions, or flooding. For example, this dataset does not include frozen water bodies.

Therefore, we recommend using evaluations from multiple independent datasets from various sources to achieve further robustness in evaluation. While our dataset is primarily designed for validation purposes, it can still be used for fine-tuning pretrained models. However, it does not include the original input PlanetScope images of our labels, which are required for training models. This ensures that there is no data leak from the training process, maintaining the integrity of the evaluation process. Nevertheless, relying on a single dataset for evaluation has its limitations, and using multiple independent datasets is crucial for assessing the robustness and generalizability of surface water mapping methods.

5 Data availability

Our global surface water dataset used in this study is available in the CyVerse Data Commons, accessible via https://doi.org/10.25739/03nt-4f29 (Mukherjee et al., 2024).

6   Discussion and conclusions

In this study, we have presented a globally sampled, high-resolution surface water dataset consisting of 100 hand-labeled images derived from 3 m PlanetScope imagery. Our dataset covers diverse biomes and contexts, including urban and rural areas, lakes, rivers, braided rivers, and coastal regions. The thorough labeling process, which involves cross-referencing multiple data sources and extensive quality control, ensures the reliability of the labels. These characteristics make our dataset a valuable resource for evaluating the performance and robustness of surface water mapping methods across a wide range of landscapes.

By applying our dataset to the S2-based Dynamic World and S1-based NASA IMPACT models, we demonstrated its utility in identifying the strengths and limitations of different satellite imagery products and methodologies. The variability in performance across biomes highlights the importance of using representative validation data to assess the spatial generalizability of mapping methods. Our findings underscore the need for multiple independent validation datasets to comprehensively evaluate surface water products and build trust in their results.

Accurate and reliable monitoring of surface water resources is crucial for sustainable water management, climate change adaptation, and conservation efforts. High-quality validation datasets like ours play a vital role in advancing these goals by enabling the development and assessment of more effective mapping methods. We anticipate that our dataset will contribute to improving the accuracy, robustness, and spatial generalizability of surface water mapping products, ultimately supporting better-informed decision-making and more efficient management of our precious water resources in the face of growing global challenges.

Author contributions. RM, FP, and BT designed the dataset, developed the sampling strategy, and structured the paper. RM and JG wrote the paper. RW, PS, and EAT labeled the images. RM, RW, PS, EAT, and ZZ processed the data. ZZ uploaded the dataset.

References

Acharki, S.: PlanetScope contributions compared to Sentinel-2, and Landsat-8 for LULC mapping, Remote Sensing Applications: Society and Environment, 27, 100774, https://doi.org/10.1016/j.rsase.2022.100774, 2022.

Alemohammad, H. and Booth, K.: LandCoverNet: A global benchmark land cover classification training dataset, arXiv [preprint], arXiv:2012.03111, 2020.

Bamber, J. and Bindschadler, R.: An improved elevation dataset for climate and ice-sheet modelling: validation with satellite imagery, Ann. Glaciol., 25, 439–444, 1997.

Bijeesh, T. and Narasimhamurthy, K.: Surface water detection and delineation using remote sensing images: A review of methods and algorithms, Sustainable Water Resour. Manag., 6, 1–23, 2020.

Bonafilia, D., Tellman, B., Anderson, T., and Issenberg, E.: Sen1Floods11: A georeferenced dataset to train and test deep learning flood algorithms for Sentinel-1, 2020 IEEE/CVF Conference on Computer Vision and Pattern Recognition Workshops (CVPRW), Seattle, WA, USA, 835–845, https://doi.org/10.1109/CVPRW50498.2020.00113, 2020.

Brown, C. F., Brumby, S. P., Guzder-Williams, B., Birch, T., Hyde, S. B., Mazzariello, J., and Tait, A. M.: Dynamic World, Near real-time global 10 m land use land cover mapping, Sci. Data, 9, 251, https://doi.org/10.1038/s41597-022-01307-4, 2022.

Chesapeake Bay Program: Chesapeake Bay Land Use and Land Cover (LULC) Database 2022 Edition, U.S. Geological Survey data release, https://doi.org/10.5066/P981GV1L, 2023.

Cloud to Street, Microsoft, and Radiant Earth Foundation: A Global Flood Events and Cloud Cover Dataset (Version 1.0), https://registry.opendata.aws/c2smsfloods/ (last access: 9 September 2024), 2022.

Dai, A.: Increasing drought under global warming in observations and models, Nat. Clim. Change, 3, 52–58, 2013.

Gahlot, S., Gurung, I., Molthan, A., Maskey, M., and Ramasubramanian, M.: Flood Extent Data for Machine Learning, Radiant MLHub [data set], https://doi.org/10.34911/rdnt.ebk43x, 2021.

Ghayour, L., Neshat, A., Paryani, S., Shahabi, H., Shirzadi, A., Chen, W., Al-Ansari, N., Geertsema, M., Pourmehdi Amiri, M., Gholamnia, M., Dou, J., and Ahmad, A.: Performance evaluation of sentinel-2 and landsat 8 OLI data for land cover/use classification using a comparison between machine learning algorithms, Remote Sens., 13, 1349, https://doi.org/10.3390/rs13071349, 2021.

Giezendanner, J., Mukherjee, R., Purri, M., Thomas, M., Mauerman, M., Islam, A. K. M. S., and Tellman, B.: Inferring the Past: A Combined CNN-LSTM Deep Learning Framework To Fuse Satellites for Historical Inundation Mapping, 2155–2165, https://doi.org/10.1109/CVPRW59228.2023.00209, 2023.

Isikdogan, F., Bovik, A. C., and Passalacqua, P.: Surface water mapping by deep learning, IEEE J. Sel. Top. Appl. Earth Obs., 10, 4909–4918, 2017.

Labelbox: Online platform for data labeling, https://labelbox.com (last access: 15 March 2024), 2024.

Li, J., Ma, R., Cao, Z., Xue, K., Xiong, J., Hu, M., and Feng, X.: Satellite detection of surface water extent: A review of methodology, Water, 14, 1148, https://doi.org/10.3390/w14071148, 2022.

Markert, K. N., Chishtie, F., Anderson, E. R., Saah, D., and Griffin, R. E.: On the merging of optical and SAR satellite imagery for surface water mapping applications, Results in Physics, 9, 275–277, 2018.

Martinis, S.: Improving flood mapping in arid areas using Sentinel-1 time series data, in: 2017 IEEE International Geoscience and Remote Sensing Symposium (IGARSS), IEEE, 193–196, https://doi.org/10.1109/IGARSS.2017.8126927, 2017.

Martinis, S., Groth, S., Wieland, M., Knopp, L., and Rättich, M.: Towards a global seasonal and permanent reference water product from Sentinel-1/2 data for improved flood mapping, Remote Sens. Environ., 278, 113077, https://doi.org/10.1016/j.rse.2022.113077, 2022.

Misra, I., Lawrence Zitnick, C., Mitchell, M., and Girshick, R.: Seeing through the human reporting bias: Visual classifiers from noisy human-centric labels, in: Proceedings of the IEEE conference on computer vision and pattern recognition, 2930–2939, https://doi.org/10.48550/arXiv.1512.06974, 2016.

Mueller, N., Lewis, A., Roberts, D., Ring, S., Melrose, R., Sixsmith, J., Lymburner, L., McIntyre, A., Tan, P., Curnow, S., Ip, A.: Water observations from space: Mapping surface water from 25 years of Landsat imagery across Australia, Remote Sens. Environ., 174, 341–352, https://doi.org/10.1016/j.rse.2015.11.003, 2016.

Mukherjee, R., Zhang, Z., Policeli, F., Wang, R., and Tellman, B.: Rohit_GlobalSurfaceWaterDataset_2024, CyVerse Data Commons [data set], https://doi.org/10.25739/03nt-4f29, 2024.

Olson, D. M., Dinerstein, E., Wikramanayake, E. D., Burgess, N. D., Powell, G. V. N., Underwood, E. C., D'amico, J. A., Itoua, I., Strand, H. E., Morrison, J. C., Loucks, C. J., Allnutt, T. F., Ricketts, T. H., Kura, Y., Lamoreux, J. F., Wettengel, W. W., Hedao, P., and Kassem, K. R.: Terrestrial ecoregions of the world: A new global map of terrestrial ecoregions provides an innovative tool for conserving biodiversity, BioScience, 51, 933–938, https://doi.org/10.1641/0006-3568(2001)051[0933]2.0.CO;2, 2001.

Patterson, T. and Kelso, N. V.: World Urban Areas, LandScan, 1 : 10 million (2012) [Shapefile], North American Cartographic Information Society, https://earthworks.stanford.edu/catalog/stanford-yk247bg4748 (last access: 12 February 2024), 2012.

Paul, S. and Ganju, S.: Flood segmentation on sentinel-1 SAR imagery with semi-supervised learning, arXiv [preprint], arXiv:2107.08369, 2021.

Paullada, A., Raji, I. D., Bender, E. M., Denton, E., and Hanna, A.: Data and its (dis) contents: A survey of dataset development and use in machine learning research, Patterns, 2, 100336, https://doi.org/10.1016/j.patter.2021.100336, 2021.

Pekel, J.-F., Cottam, A., Gorelick, N., and Belward, A. S.: High-resolution mapping of global surface water and its long-term changes, Nature, 540, 418–422, 2016.

Planet Team: Planet application program interface: In space for life on Earth, San Francisco, CA, 2017, 2, 2017.

Rambour, C., Audebert, N., Koeniguer, E., Le Saux, B., Crucianu, M., and Datcu, M.: Flood detection in time series of optical and sar images, The International Archives of the Photogrammetry, Remote Sens. Spatial Inf. Sci., 43, 1343–1346, 2020.

Sumbul, G., Charfuelan, M., Demir, B., and Markl, V.: Bigearthnet: A large-scale benchmark archive for remote sensing image understanding, in: IGARSS 2019–2019 IEEE International Geoscience and Remote Sensing Symposium, Yokohama, Japan, 28 July–2 August, 5901–5904, IEEE, 2019.

Tellman, B., Sullivan, J., Kuhn, C., Kettner, A., Doyle, C., Brakenridge, G., Erickson, T., and Slayback, D.: Satellite imaging reveals increased proportion of population exposed to floods, Nature, 596, 80–86, 2021.

Vandewiele, G., Dehaene, I., Kovács, G., Sterckx, L., Janssens, O., Ongenae, F., De Backere, F., De Turck, F., Roelens, K., Decruyenaere, J., Van Hoecke, S., and Demeester, T.: Overly optimistic prediction results on imbalanced data: a case study of flaws and benefits when applying oversampling, Artificial Intelligence in Medicine, 111, 101987, https://doi.org/10.1016/j.artmed.2020.101987, 2021.

Wieland, M., Martinis, S., Kiefl, R., and Gstaiger, V.: Semantic segmentation of water bodies in very high-resolution satellite and aerial images, Remote Sens. Environ., 287, 113452, https://doi.org/10.1016/j.rse.2023.113452, 2023.

Wolpert, D. H.: The supervised learning no-free-lunch theorems, in: Soft computing and industry: Recent applications, edited by: Roy, R., Köppen, M., Ovaska, S., Furuhashi, T., and Hoffmann, F., Soft Computing and Industry, Springer, London, 39–66, https://doi.org/10.1007/978-1-4471-0123-9_3, 2002.

World Wildlife Fund: Global Lakes and Wetlands Database: Large Lake Polygons (Level 1), https://www.worldwildlife.org/publications/global-lakes-and-wetlands-database-large-lake-polygons-level-1 (last access: 12 February 2024), 2005.

Wulder, M. A., Hilker, T., White, J. C., Coops, N. C., Masek, J. G., Pflugmacher, D., and Crevier, Y.: Virtual constellations for global terrestrial monitoring, Remote Sens. Environ., 170, 62–76, 2015.

https://doi.org/10.5194/essd-16-4311-2024

Earth Syst. Sci. Data, 16, 4311–4323, 2024